Acta Pharmaceutica Sinica B 2019;9(3):615–625

Chinese Pharmaceutical Association
Institute of Materia Medica, Chinese Academy of Medical Sciences

Acta Pharmaceutica Sinica B

www.elsevier.com/locate/apsb
www.sciencedirect.com

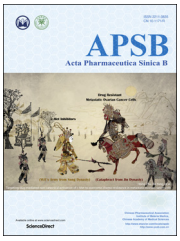

ORIGINAL ARTICLE

Overcoming chemotherapy resistance *via* simultaneous drug-efflux circumvention and mitochondrial targeting

Minglu Zhou[a], Lijia Li[a], Lian Li[b], Xi Lin[a], Fengling Wang[a], Qiuyi Li[a], Yuan Huang[a,*]

[a]*Key Laboratory of Drug Targeting and Drug Delivery System (Ministry of Education), West China School of Pharmacy, Sichuan University, Chengdu 610041, China*
[b]*Department of Pharmaceutics and Pharmaceutical Chemistry/Center for Controlled Chemical Delivery, University of Utah, Salt Lake City, UT 84112, USA*

Received 15 July 2018; received in revised form 17 September 2018; accepted 26 October 2018

KEY WORDS

Drug resistance;
P-gp pumps;
Mitochondrial targeting;
HPMA copolymer;
Drug delivery;
Doxorubicin

Abstract Multidrug resistance (MDR) has been considered as a huge challenge to the effective chemotherapy. Therefore, it is necessary to develop new strategies to effectively overcome MDR. Here, based on the previous research of *N*-(2-hydroxypropyl)methacrylamide (HPMA) polymer–drug conjugates, we designed an effective system that combined drug-efflux circumvention and mitochondria targeting of anticancer drug doxorubicin (Dox). Briefly, Dox was modified with mitochondrial membrane penetrating peptide (MPP) and then attached to (HPMA) copolymers (P-M-Dox). Our study showed that macromolecular HPMA copolymers successfully bypassed drug efflux pumps and escorted Dox into resistant MCF-7/ADR cells *via* endocytic pathway. Subsequently, the mitochondria accumulation of drugs was significantly enhanced with 11.6-fold increase by MPP modification. The excellent mitochondria targeting then resulted in significant enhancement of reactive oxygen species (ROS) as well as reduction of adenosine triphosphate (ATP) production, which could further inhibit drug efflux and resistant cancer cell growth. By reversing Dox resistance, P-M-Dox achieved much better suppression in the growth of 3D MCF-7/ADR tumor spheroids compared with free Dox. Hence, our study provides a promising approach to treat drug-resistant cancer through simultaneous drug efflux circumvention and direct mitochondria delivery.

*Corresponding author. Tel.: +86 28 85501617.
E-mail address: huangyuan0@163.com (Yuan Huang).

Peer review under responsibility of Institute of Materia Medica, Chinese Academy of Medical Sciences and Chinese Pharmaceutical Association.

https://doi.org/10.1016/j.apsb.2018.11.005

1. Introduction

Multidrug resistance (MDR) has been considered as the main obstacle limiting the success of anticancer chemotherapy[1–5]. The mechanisms underlying multidrug resistance are multifactorial, but largely involve the P-glycoprotein (P-gp) that pumps drug out and results in intracellular sub-lethal drug concentration[6,7]. P-gp is commonly overexpressed in various cancers and can be further upregulated after exposure to anticancer drugs[8,9]. Up to 50% of widely used chemotherapeutics, for instance, doxorubicin, paclitaxel and docetaxel, are P-gp substrates and cancer cells can easily develop cross-resistance to these drugs[10,11]. Most recent developments in anti-MDR strategies include P-gp inhibitors[12], RNA-silencing[13], nanopreparations[14] and co-administration strategies[15]. Despite these strategies have achieved some effects in previous studies, their clinical administration are still hampered by several impediments, including non-specific action, individual difference, intolerable side effects and expensive cost[16,17]. Therefore, considerable efforts have been made to inhibit P-gp function for tackling MDR.

Most free drugs enter cells by diffusion. As such, they are extremely susceptible to efflux pumps on the cell membrane[18]. On the contrary, macromolecules are internalized by cells through endocytosis[19–21]. Some studies have proved polymer and nanoparticle based delivery systems can bypass P-gp efflux[22,23]. It has been reported that *N*-(2-hydroxypropyl) methacrylamide (HPMA) copolymer doxorubicin (Dox) conjugates could partially reduce drug efflux in Dox-resistant human ovarian carcinoma A2780/AD cells[24]. In contrast to free Dox, HPMA copolymer containing doxorubicin (Dox) did not show remarkably reduced cytotoxicity in resistant cells, as compared with the sensitive cells. The result was attributed to that the internalization of these conjugates were dependent on endocytosis and helped Dox escape the P-gp efflux pump.

In addition, delivering anticancer drugs to mitochondria provides a new opportunity to overcome MDR[25,26]. On one hand, adenosine triphosphate (ATP) is essential for the function of P-gp pumps, and direct attack towards mitochondria, the major "powerhouse" of cells, cuts off their energy supply[27,28]; on the other hand, the dysfunction of mitochondria can disrupt the intracellular metabolism, activate mitochondrial apoptotic pathways and eventually kill the tumor cells[29]. However, it remains challenging for most macromolecules including HPMA copolymers to achieve mitochondrial targeting, due to the numerous intracellular barriers[30,31]. In particular, the extremely low permeability of the mitochondrial inner membrane hinders drugs from entering into the interior of the mitochondria[32]. Recently, Horton et al.[33] designed and synthesized a novel mitochondrial membrane penetrating peptide (MPP, FXrFXKFXrFXK) based on the balance between cation parameters and hydrophobicity. Compared to the cell penetrating peptides (CPPs), MPP was additionally introduced with hydrophobic amino acids to better interact with the mitochondrial membrane with more hydrophobic nature. By adjusting the ratio of cationic amino acids R and K (arginine and lysine) and hydrophobic amino acid Fx (cyclohexylalanine), MPP not only maintains the ability of CPPs to enhance cellular uptake, but also exhibits mitochondrial targeting ability[34]. Up to now, it has been demonstrated that chlorambucil (an anti-tumor drug) covalently tagged with MPP substantially accumulated in mitochondria[35].

Herein, based on previous achievements, we rationally design a polymeric platform that combines the function of P-gp evasion and mitochondrial targeting in order to reverse drug resistance. Different from other common strategies[36,37] for overcoming drug resistance (combination therapy[38] and gene therapy[39]) with complex system to compromise the interaction, different property and distinct release behavior between agents, the system consists of an MPP as a mitochondria targeting moiety; HPMA copolymers as carriers[40–43]; doxorubicin as a model drug and hydrazone bond as a pH-sensitive linker. We expect the mitochondria-targeting HPMA copolymer–doxorubicin conjugates (P-M-Dox) could enter cells through endocytosis to bypass p-gp efflux pumps, then release MPP-modified doxorubicin (M-Dox) in responsive to the lysosomal acidic environment, and eventually target mitochondria to minimize the production of ATP and activate mitochondria-mediated apoptotic pathways, thereby overcoming MDR in tumor cells (Fig. 1).

2. Materials and methods

2.1. Materials

Doxorubicin hydrochloride (DOX · HCl) was purchased from Dalian Meilun Biotech Co., Ltd. (Dalian, China). Mitochondria penetration peptide (MPP: HS–FxrFxKFxrFxK) was synthesized by Taopu Biology Technology Co., Ltd. (Shanghai, China). Glycylglycine (GG) and *N*-succinimidyl-3-maleimidopropionate (SMP) was purchased from J&K Co., Ltd. (shanghai, China). 1-[3-(Dimethylamino)propyl]-3-ethylarbodiimide hydrochloride (EDC · HCl) was gained from Meapeo Co., Ltd. (Shanghai, China). 3-(4,5-Dimethyl-2-tetrazolyl)-2,5-diphenyl-2*H* tetrazoliumbromide (MTT) and 4′,6-diamidino-2-phenylindole (DAPI) were purchased from Sigma–Aldrich (St. Louis, MO, USA). Mitotracker Green was purchased from Invitrogen (Carlsbad, CA, USA). All other chemicals and reagents were of analytical grade.

2.2. Synthesis of monomers

The monomers of *N*-(2-hydroxypropyl) methacrylamide (HPMA) and *N*-methacryloyl-glycylglycine (MA-GG–OH) were synthesized according to previous reports[44,45]. *N*-Methacryloyl-glycyl-glycyl-hydrazide (MA-GG–$NHNH_2$) and the pH-sensitive *N*-methacryloyl-glycylglycyl-hydrazide-doxorubicin (MA-GG–NHN=DOX) were synthesized as following described[33]: MA-GG–OH (2.1 mmol), 4-dimethylaminopyridine (DMAP), and *N*, *N*′-dicyclohexylcarbodiimide (DCC, 4.0 mmol) were dissolved in ethanol and stirred for 2 h at 0 °C and for another 2 h at room temperature. After filtration, the filtrate was collected and stirred with hydrazinium hydroxide for 4 h. Hexanol was added to produce precipitation. Then the white precipitation, MA-GG–$NHNH_2$, was gained after filtration and washed with the mixture of hexanol and ethanol. Then the obtained MA-GG–$NHNH_2$ (1 mmol) was mixed with doxorubicin hydrochloride (1 mmol) and dissolved in methanol (100 mL) and acetic acid (5 mL). After reacting at room temperature for 48 h, the solvent was evaporated and vacuum dried to obtain red sediment of MA-GG–NHN=DOX with an 82.5% yield. ^{1}H NMR (400 MHz, DMSO-d_6): d (ppm) ¼ 4.97 (d, 1H), 5.37 (s, 1H), 5.73 (s, 1H), 7.65 (s, 1H), 7.91 (s, 1H), 8.03(s, 1H), 8.22 (s, 1H), 8.36 (s, 1H), 10.67 (s, 1H), 11.26 (s, 1H); MS: $C_{35}H_{41}N_5O_{13}$, 740.3 $[M+H]^+$.

2.3. Synthesis of MPP–doxorubicin conjugates

MPP–doxorubicin conjugate (M-Dox) was synthesized as follows. At first, Dox was reacted with *N*-succinimidyl-3-

maleimidopropionate (SMP). Briefly, Dox (21.8 mg), SMP (11.0 mg), and triethylamine (TEA, 21 μL) were dissolved in 4 mL of dimethylformamide (DMF) and stirred for 2 h at room temperature in the dark. The reaction solution was purified by precipitating and washing twice with cold anhydrous diethyl ether. After centrifugation, the red sediment was collected and vacuum dried. Then, Dox–SMP was dissolved in 0.25 mL DMF and mixed with a solution of MPP (HS–FxrFxKFxrFxK, 6.75 mg) dissolved in 0.25 mL *N*,*N*-dimethylformamide (DMF) and 10 μL trimethylamine (TEA). After 2 h, the sample was purified with the addition of cold anhydrous diethyl ether, centrifuged and vacuum dried to obtain the product with an 81% yield in red crystals.

2.4. Synthesis of polymeric conjugates

The MPP modified HPMA copolymer–doxorubicin conjugate (P-M-Dox) was synthesized by three steps. At first, HPMA copolymer–doxorubicin conjugate (P-Dox) was synthesized by radical solution polymerization[45]. Briefly, HPMA monomer, MA-GG–NHN=Dox (HPMA:MA-GG–NHN=Dox = 92.5:7.5, mol/mol) and AIBN as initiator were dissolved in anhydrous methanol (polymer monomer:initiator:solvent = 12.5:2:85.5, *w*/*w*/*w*). The mixture was polymerized at 50 °C for 24 h under the protection of argon. After reaction, the polymer was precipitated in diethyl ether, purified by dialysis, and then dried under vacuum. Then P-Dox, SMP (1:4, mol/mol) and TEA were dissolved in DMF and stirred for 4 h at room temperature. The reaction solution was transferred to a dialysis bag with a molecular weight of 10,000–14,000 for 48 h, and the red sponge solid P-Dox-SMP was obtained after freeze-drying in the yield of 72.4%. At last, the obtained P-Dox-SMP and MPP were co-dissolved in 4 mL PBS (pH 6.99), stirred for 48 h at room temperature in the protection of nitrogen, purified by dialysis at 4 °C, and lyophilized to obtain the final P-M-Dox product as red powder.

2.5. Characterization of polymeric conjugates

The molecular weight and polydispersity index (PDI) of the conjugates were detected by fast protein liquid chromatography system (AKTA purifier, GE Healthcare Life Science, Piscataway, NJ, USA) equipped with a Superose 6 10/300 GL column (GE Healthcare Life Science, Piscataway, NJ, USA) and a differential refraction detector (KNAUER, 2300, Germany). For this experiment, phosphate buffer (pH 7.4) was applied as mobile phase at a flow rate of 0.5 mL/min. Chromatography was performed at 25 °C. MPP content of the conjugates was detected by amino acid analysis. The content of Dox in conjugates was determined by UV–Vis spectrometry using the absorbance wavelength at 481 nm.

2.6. In vitro drug release

To measure the drug release profile under the condition of different pH (pH 7.4, 6.8, and 5.0), the conjugates were synthesized and dissolved in above mentioned phosphate buffer (pH 7.4, equivalent Dox concentration: 3 mg/mL). Furthermore, 2 mL of the above Dox-loaded conjugate solutions were dialyzed in 50 mL of corresponding phosphate buffer (37 °C, pH 7.4, 6.8, and 5.0). Free Dox solution was prepared as control. At predetermined time points (0.5, 1, 3, 5, 7, 9, 11, 24, 36, and 48 h), 100 μL of external buffer was taken out, and the fluorescence intensity of Dox was determined by Varioskan Flash (ThermoFisher Scientific, Waltham, MA, USA) at excitation wavelength of 485 nm and an emission wavelength of 590 nm. Each assay was repeated in triplicate. The release of Dox was calculated according to the measured data.

2.7. Cell culture

Human cell line HeLa (the Cell Bank of Chinese Academy of Sciences, Shanghai, China) was grown in Dulbecco's modified Eagle's medium (DMEM) supplemented with 10% fetal bovine serum and 1% antibiotics (penicillin and streptomycin). Human breast cancer cell line MCF-7 (iCell Bioscience Inc, Shanghai, China), adriamycin-resistant variant human breast cancer cell line MCF-7/ADR (iCell Bioscience Inc, Shanghai, China) were cultured in RPMI-1640 medium supplemented with 10% fetal bovine serum and 1% antibiotics (penicillin and streptomycin). To maintain the drug-resistant phenotype of MCF-7/ADR, the culture media was further supplemented with 1 μg/mL doxorubicin. All the cells were incubated at 37 °C under the air atmosphere of 5% CO_2.

2.8. Cellular uptake of the polymeric conjugates

For quantitative analysis of cellular uptake, HeLa, MCF-7, MCF-7/ADR were seeded in 12-well plates at the density of 1×10^5 cells/well and incubated under the condition of 5% CO_2 at 37 °C for 24 h. The cells were treated with P-M-Dox, P-Dox and Dox, which were dissolved and diluted with culture media to reach a final doxorubicin concentration of 10 μg/mL. The blank medium was added as control group. After 2 or 4 h incubation, cells were washed twice with cold PBS solution, treated with 0.25% trypsin–EDTA, harvested by centrifugation, and then re-suspended in PBS solution. Finally, the quantification of cellular uptake was measured using flow cytometer.

For qualitative analysis, Hela, MCF-7, MCF-7/ADR cells were seeded onto the coverslips, and then treated with P-M-Dox, P-Dox and Dox (equivalent Dox dose of 10 μg/mL) for 4 h. After rinsed with cold PBS, cells were fixed with 4% paraformaldehyde and stained with DAPI (5 μg/mL) for 5 min. The fluorescence images were observed by confocal laser scanning microscopy.

2.9. Dox efflux assay

The efflux of Dox was estimated in MCF-7 and MCF-7/ADR cells. After treated with P-M-Dox, P-Dox, Dox (equivalent Dox dose, 10 μg/mL) for 4 h, cells were washed and further incubated with fresh medium for another 2 h and 4 h at 37 °C. Then, cells were collected and washed with PBS to remove the extracellular Dox. The fluorescence of DOX retained in cells was detected by flow cytometer.

2.10. Calcein efflux assay

Calcein-AM is one of the substrate of P-gp, which means the function of P-gp will lead to extrusion of calcein-AM and less intracellular accumulation of calcein (calcein-AM is hydrolyzed

into calcein after entering cells)[46,47]. Therefore the activity of P-gp can be reflected by detecting the fluorescence of retained calcein in cells. In order to investigate the mechanism of drug efflux of MCF-7/ADR cells, the P-gp activity of MCF7/ADR and MCF-7 were compared. Cells were cultured in 12 well plates at 37 °C for 24 h. Then, cells were treated with 0.2 μmol/L calcein AM in dark for 30 min. After the incubation period, cells were washed with PBS, centrifuged, and then resuspended in cold PBS. Finally, the fluorescence of the accumulated calcein was determined by flow cytometer. Weaker fluorescence represented stronger activity of P-gp.

To further study the probable effect of P-M-Dox, P-Dox, Dox on p-gp activity, MCF-7 and MCF-7/ADR cells were cultured in 12 well plates at 37 °C for 24 h. Afterwards, cells were treated with above mentioned samples (equivalent Dox dose, 10 μg/mL) for 18 h. After being washed twice with cold PBS, cells were incubated with 0.2 μmol/L calcein AM in dark for another 30 min. Then cells were collected and washed to remove the extracellular Calcein and detected by flow cytometer.

2.11. Cellular uptake mechanism assays of polymeric conjugates

To further identity the possible endocytosis pathways of P-M-Dox, Hela, MCF-7, MCF-7/ADR cells were cultured into 24 well plates. After 24 h incubation, cells were cultured at 4 °C or in the prepared solution of different endocytosis inhibitors at 37 °C for 1 h. Sodium azide (1 mg/mL), lovastatin (10 μg/mL), chlorpromazine (10 μg/mL), amiloride (0.3 mg/mL) were used as active transport inhibitors. In addition, the control group was the culture in the absence of inhibitor. To further estimate the effect of temperature on internalization, the experiment was also performed at 4 °C for 2 h without any treatment. Then cells were washed twice with cold PBS and following treated with P-M-Dox, P-Dox (equivalent Dox dose, 10 μg/mL). After 2 h incubation, cells were washed with cold PBS solution, centrifuged and re-suspended in PBS solution. The inhibition rate was expressed as the percentage of that internalized in control.

2.12. Mitochondria targeting

Laser confocal scanning fluorescent microscopy was used to observe the co-localization of drug with the mitochondria. HeLa, MCF-7, MCF-7/ADR cells were seeded onto the coverslips in the 12 wells plates for 24 h, and then treated with P-M-Dox, P-Dox, Dox (equivalent Dox dose, 10 μg/mL) for 4 h. After rinsed three times with cold PBS, cells were further incubated with Mitotracker Green FM (100 nmol/L) for another 45 min. Then cells were fixed with 4% paraformaldehyde and further treated with DAPI (5 μg/mL).

Simultaneously, the quantitative experiment was performed by flow cytometer. HeLa, MCF-7, MCF-7/ADR cells were seeded in 12 wells plates and then treated with P-M-Dox, P-Dox, Dox (equivalent Dox dose, 10 μg/mL). The cells were collected and suspended in the mitochondria extraction reagent under the condition of ice bath for 10 min. The suspensions were further homogenated with homogenizer. After being centrifuged (600 × *g*, 10 min), the supernatants were collected and further centrifuged (11,000 × *g*, 10 min). Then, precipitated mitochondria were collected. Dox accumulated in mitochondria was analyzed by flow cytometer.

2.13. Specific mitochondria damage after subcellular targeting

Intracellular ROS level is often considered as important index of damaged mitochondria[47]. To measure the changes in ROS level, 2′,7′-dichlorofluorescein diacetate (DCFH-DA) was applied[48]. Briefly, HeLa, MCF-7, MCF-7/ADR cells were pre-treated with P-M-Dox, P-Dox, Dox (equivalent Dox dose, 10 μg/mL) for 6 h. According to the instruction, cells were then harvested and incubated with DCFH-DA (10 μmol/L) in the dark. After 25 min incubation, cells were washed with fresh culture medium without fetal bovine serum (FBS), centrifuged and re-suspended in PBS solution. Finally, the intracellular ROS level was estimated for measuring green fluorescence by flow cytometer.

2.14. Intracellular ATP assay

The intracellular ATP levels were measured using a luciferase-based ATP assay kit (Beyotime, China). MCF-7/MDR cells at a density of 5×10^4 cells/well were seeded in 24-well plates, and then incubated with different formulation (P-M-Dox, P-Dox, Dox, equivalent Dox dose, 10 μg/mL) for 12 h. According to the instruction, cells were lysed and centrifuged at 12,000 × *g* for 5 min. The supernatant was collected and mixed with the ATP detection working dilution in a ratio of 1:5. The luminescence intensity was detected by microplate reader (Bio-Rad, Microplate Reader 550).

2.15. Cytotoxicity assay

The *in vitro* cytotoxicity of polymeric conjugates against Hela, MCF-7, MCF-7/ADR cells was examined by MTT assay. Cells were seeded in 96-well plates for 24 h at 37 °C, and then treated with P-M-Dox, P-Dox and Dox in dose equivalent to 0.15–50 μg/mL of Dox. After 24 and 48 h incubation, MTT solution (20 μL, 5 mg/mL) were added and incubated for another 4 h. After removing the solution, 180 μL DMSO were added and incubated for 30 min to dissolve the formazan. The absorbance was measured at 570 nm wavelength by microplate reader microplate reader (Bio-Rad, Microplate Reader 550). The cell viability was calculated. Each assay was repeated in triplicate.

2.16. Inhibition of tumor spheroids growth

To mimic solid tumor, three-dimensional tumor spheroids of HeLa, MCF-7 and MCF-7/ADR cells were established as previously described[49,50]. Cells (1500 cells/well) were seeded in a 96-well plate pre-coated with 2% (*w*/*v*) agarose gel. After 3 days incubation, the spheroids with uniform size and compact structure were exposed to Dox, P-Dox and P-M-Dox (equivalent Dox concentration of 10 mg/mL) with a drug-free group as control. The maximum (d_{max}) and minimum (d_{min}) diameter of each spheroid was monitored for 7 days. The volume was calculated with the following formula: $V = (\pi \times d_{max} \times d_{min})/6$. The change ratio of the tumor spheroids volume was presented as the percentage of original volume prior to treatment.

2.17. Statistical analysis

Results were expressed as the means ± SD. Differences between groups were analyzed by using SPSS 22.0 software (Chicago, IL, USA). The Statistically significant difference was defined as $P < 0.05$ and highly significant difference was defined as $P < 0.01$.

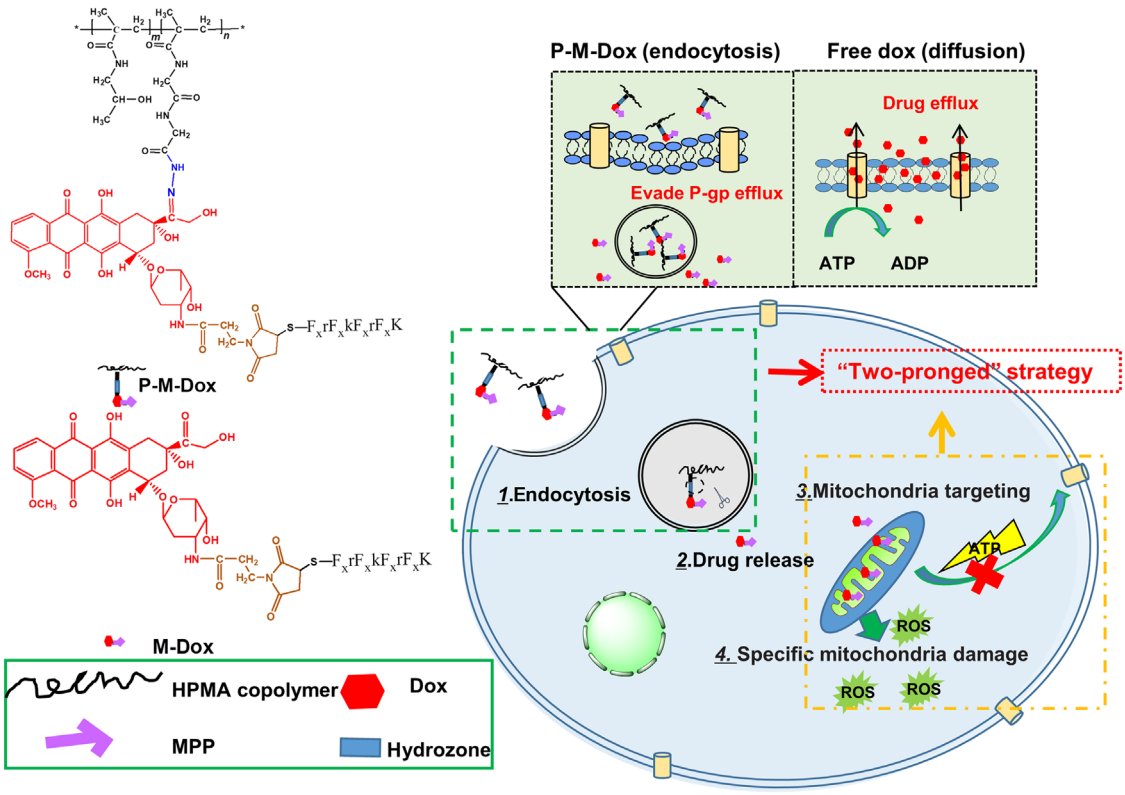

Figure 1 Schematic illustration of P-M-Dox to overcome multidrug resistance *via* simultaneous drug-efflux circumvention and mitochondrial targeting. Free Dox that enter cells by diffusion is vulnerable to P-gp efflux. On the contrary, P-M-Dox that enters cells by endocytosis can effectively evade P-gp efflux pump on the cell membrane. Then, P-M-Dox responsively releases MPP modified doxorubicin (M-Dox) in the lysosomal acidic environment, and eventually achieves excellent mitochondria targeting for elevating ROS generation and minimizing ATP production, thereby killing drug-resistant tumor cells.

3. Result and discussion

3.1. Macromolecular HPMA vehicle bypasses drug efflux in resistant cells

The mitochondria-targeting HPMA copolymer-doxorubicin conjugates (P-M-Dox) with pH sensitivity were successfully synthesized by three steps (Supporting Information Scheme S1). First, HPMA copolymer–doxorubicin conjugates (P-Dox) were polymerized through radical solution polymerization as previously reported[45]. Then the 3′ amino group of Dox was reacted with the active ester group of SMP to obtain P-Dox-SMP. To confer mitochondria targeting ability, P-Dox was further attached with MPP *via* Michael addition action (P-M-Dox). Both polymeric conjugates showed similar characteristics with previous description[51,52], which preliminarily formed the basis for their potential in bioavailability and biosafety. Supporting Information Table S1 summarized the characterizations of products in each step. As for P-M-Dox, the molecular weight was measured as 22.3 kDa with PDI of 1.89. The Dox and MPP loading were 11.09% (*w*/*w*) (5 Dox molecules per polymer chain) and 129.6 μmol/g (3 MPP moiety per polymer chain), respectively.

To verify whether the attachment of Dox to macromolecular HPMA copolymer circumvented the P-gp pumps in resistant cells, we first investigated and compared the cell uptake in both sensitive MCF-7 and resistant MCF-7/ADR cells. As displayed in Fig. 2A, each group exhibited time-dependent uptake. Moreover, free Dox diffused rapidly into MCF-7 cells while it showed extremely low accumulation in MCF-7/ADR cells. In contrast, the uptake of P-M-Dox and P-Dox were not greatly affected in these two cell lines. Impressively, P-M-Dox and P-Dox exhibited 7.53-fold (4 h, $P < 0.01$) and 4.71-fold (4 h, $P < 0.01$) higher internalization than free Dox in resistant MCF-7/ADR cells. The data indicated the potential of P-M-Dox and P-Dox to facilitate cellular accumulation in drug-resistant cells. In addition, regardless of cell type, P-M-Dox showed greater internalization than P-Dox ($P < 0.01$), which might be contributed to the lipophilic and highly cationic characters of MPP[35,53].

Afterwards, the *in vitro* drug efflux assay was carried out. MCF-7 and MCF-7/ADR cells were first incubated with samples and then cultured in fresh blank medium for another 2 or 4 h. Then Dox retained in cells was determined and compared with the initial intake of the cells. After free Dox treatment, the Dox efflux rate in drug-resistant MCF-7/ADR cell was as high as 58.26% (2 h) and 84.88% (4 h), which was 1.74-fold (2 h, $P < 0.01$) and 2.08-fold (4 h, $P < 0.01$) higher than that in MCF-7 cells (Fig. 2B). Our result was consistent with previous report[54] that a large amount of free dox was pumped out from MCF-7/ADR cells. Notably, P-M-Dox and P-Dox significantly decreased Dox efflux rate to 29.2% and 41.3% (4 h) (Fig. 2B). The data verified the ability of macromolecular HPMA vehicle to efficiently alleviate drug efflux which might be directly associated with the drug resistance. In addition, only at 4 h after P-M-Dox administration, the efflux of MCF-7/ADR cells was suppressed to the level close to that of

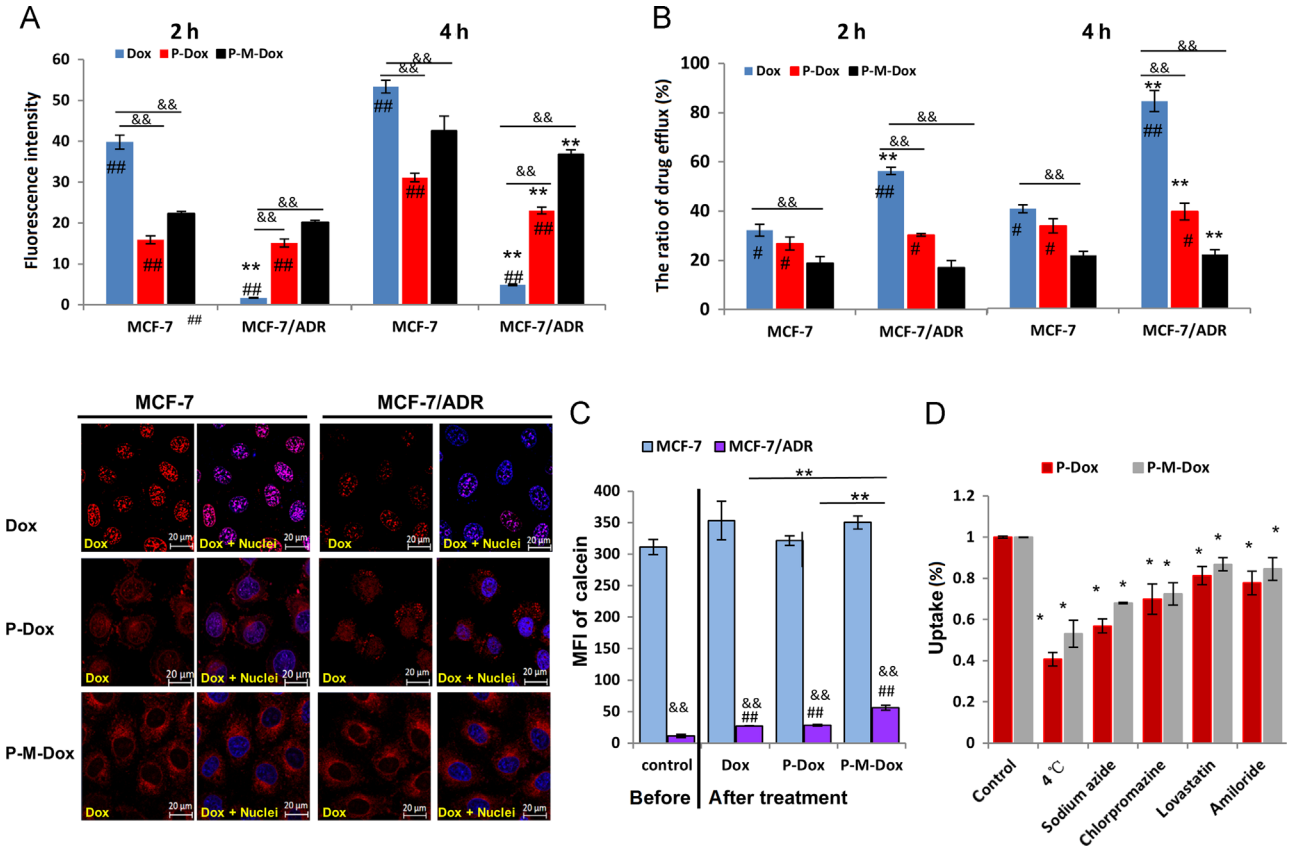

Figure 2 Macromolecular HPMA vehicle bypasses drug efflux in resistant cells. (A) Flow cytometry analysis and confocal imaging of cell uptake in MCF-7, MCF-7/ADR cells after incubation with Dox, P-Dox and P-M-Dox. Scare bar: 20 μm. Results are mean±SD, $n=3$. $^{**}P<0.01$ *versus* MCF-7 cells, $^{\#\#}P<0.01$ *versus* P-M-Dox and $^{\&\&}P<0.01$ *versus* Dox. (B) Drug efflux of Dox, P-Dox, P-M-Dox in MCF-7 and MCF-7/ADR cells. Cells were first treated with P-M-Dox, P-Dox, Dox for 4 h, and then incubated with drug-free medium for 2 or 4 h. The ratio of drug efflux was calculated by compared the retained Dox to the initial intake of the cells. Results are mean ± SD, $n=3$. $^{**}P<0.01$ *versus* MCF-7 cells; $^{\#}P<0.05$, $^{\#\#}P<0.01$ *versus* P-M-Dox and $^{\&\&}P<0.01$ *versus* Dox. (C) P-gp activity before and after drug treatment in MCF-7 and MCF-7/ADR cells. Cells were incubated with or without samples for 18 h, and then incubated with calcein–AM for another 15 min. Fluorescence intensity of retained calcein was measured by FCM. Results are mean ± SD, $n=3$. $^{**}P<0.01$ *versus* P-M-Dox, $^{\#\#}P<0.01$ *versus* control, $^{\&\&}P<0.01$ *versus* MCF-7 cells. (D) Endocytosis mechanism studies in MCF-7/ADR cells. Cells were pretreated with sodium azide, amiloride, chlorpromazine, and lovastatin for 1 h. Fluorescence intensity in the non-treated cells was used as control. The equivalent of Dox is 10 μg/mL. Results are mean±SD, $n=3$. $^{*}P<0.05$ *versus* control.

MCF-7 cells, implying the synergistic effect of MPP modification and HPMA copolymer carriers in anti-MDR activity.

We further get insight into the reason why P-M-Dox could decrease drug efflux. Due to the close relationship between drug efflux and P-gp[11,55], we determined the P-gp activity in MCF-7 and resistant MCF-7/ADR cells before or after treatment. As expected, before any treatment, the P-gp activity on MCF-7/ADR cells was 27-fold higher than that of MCF-7 cells (Fig. 2C). Notably, after treatments, the amount of calcein retained in the MCF-7/ADR cells enhanced greatly, indicating that the activity of P-gp decreased. Inspiringly, P-M-Dox showed the highest ability of P-gp suppression with 4.95-fold than control ($P < 0.01$), 2.25-fold than free Dox ($P < 0.01$) and 1.78-fold than P-Dox ($P < 0.01$), which was in accordance with drug efflux results. However, regardless of free Dox or polymer–Dox conjugates treatments, MCF-7/ADR cells still displayed much higher P-gp activities than MCF-7. Therefore we speculated P-gp inhibition was only one of the main mechanisms for the improved uptake of P-Dox and P-M-Dox in Dox resistant cells. We further examined the uptake mechanism in MCF-7/ADR cells. The results (Fig. 2D) showed the uptake of both copolymers were significantly reduced with the addition of active transport inhibitors (sodium azide) or under the condition of low temperature (4 °C), suggesting the involvement of energy-dependent transport. Also, approximately 20%–40% inhibition of cellular uptake was observed in the presence of selective inhibitors (lovastatin, chlorpromazine, amiloride) for both polymers indicating the involvements of multiple endocytosis pathways including caveolae-mediated, clathrin-mediated endocytosis and micropinocytosis[56]. In general, our results showed P-M-Dox possessed similar cell entry pathways as P-Dox, and MPP attachment did not interfere with the endocytosis process.

3.2. *MPP attachment facilitates mitochondrial drug delivery*

Afterwards, the *in vitro* drug release was studied in phosphate buffer saline with different pH values (pH 7.4, 6.8, and 5.0) simulating blood circulation, tumor environment and lysosome. As shown in Fig. 3A and Supporting Information Fig. S1, compared to free Dox, P-M-Dox and P-Dox showed similar trend with pH sensitive drug release, indicating MPP modification had no effect

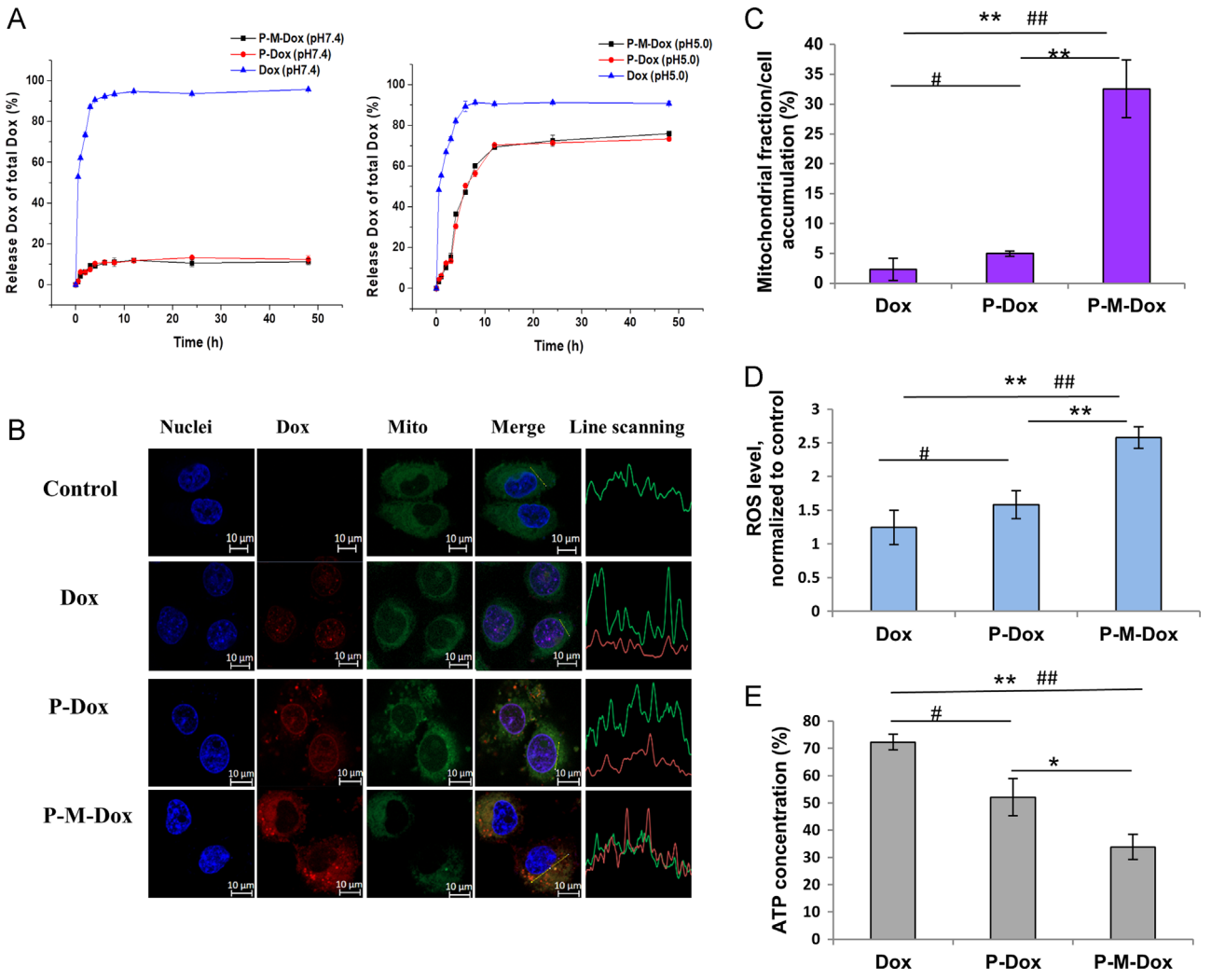

Figure 3 MPP attachment facilitates mitochondrial drug delivery. (A) *In vitro* release profile of free Dox, P-Dox and P-M-Dox in phosphate buffer saline (pH 7.4 and pH 5.0) at 37 °C. (B) Confocal imaging and (C) quantification of mitochondrial localization in MCF-7/ADR cells. Blue, red, green color shows nuclei, Dox fluorescence and mitochondria, respectively. While yellow color denotes the overlay of Dox fluorescence (red) and mitochondria staining (green). The scale bar represents 10 μm. (D) Changes of intracellular ROS generation induced by P-M-Dox, P-Dox, M-Dox, Dox. (E) Intracellular ATP level of MCF-7/MDR cells after 12 h incubation with different samples. Results are means ± SD, $n=3$. $^{\#}P<0.05$, $^{\#\#}P<0.01$ *versus* Dox group; $^{*}P<0.05$, $^{**}P<0.01$ *versus* P-M-Dox group (For interpretation of the references to color in this figure legend, the reader is referred to the web version of this article).

on drug release behavior. In details, P-M-Dox showed a slow drug release behavior reaching a plateau of only 11.24% at pH 7.4 and 18.04% at pH 6.8 in 48 h. In contrast, it underwent a fast drug release at pH 5.0. The release of Dox reached nearly 70% within 12 h and continued to increase, indicating specific drug detachment from HPMA copolymers in lysosome.

Having demonstrated that HPMA copolymer-mediated endocytosis facilitated the intracellular delivery of its attached payload *via* bypassing the P-gp pumps[24,57,58], we next determined whether further MPP modification endowed the system with mitochondrial targeting. For confocal imaging (Fig. 3B), in resistant MCF-7/ADR cells, only a small proportion of free Dox escaped the drug efflux pumps, and those entering the cells were mostly excluded from mitochondria but distributed into the nucleus owing to its own nuclear tendency. Similarly, insufficient accumulation in mitochondria was also observed after the treatment with P-Dox. The phenomenon took place in different cell lines, including HeLa, MCF-7 and drug-resistant MCF-7/ADR cell lines (Supporting Information Fig. S3). In contrast, instead of distribution in the nucleus, strong Dox fluorescence of P-M-Dox was observed to overlay with mitochondria, which indicated that MPP modification considerably altered the intracellular fate of P-M-Dox, leading to substantial mitochondrial localization. For quantitative analysis, mitochondria were isolated from cells to more precisely evaluate drug accumulation in mitochondria. Results (Fig. 3C and Supporting Information Fig. S3) were consistent with qualitative measurement that free Dox and P-Dox exhibited barely mitochondria distribution (< 5%) in mitochondria in HeLa, MCF-7 and drug-resistant MCF-7/ADR cells, while P-M-Dox achieved more excellent mitochondria uptake with 11.61-fold and 6.21-fold higher of mitochondria distribution than free Dox and P-Dox in resistant MCF-7/ADR cell, respectively. Moreover, results with drug efflux assay (Fig. 2B) showed P-M-Dox had the best effect on limiting drug efflux, which indicated mitochondria targeting

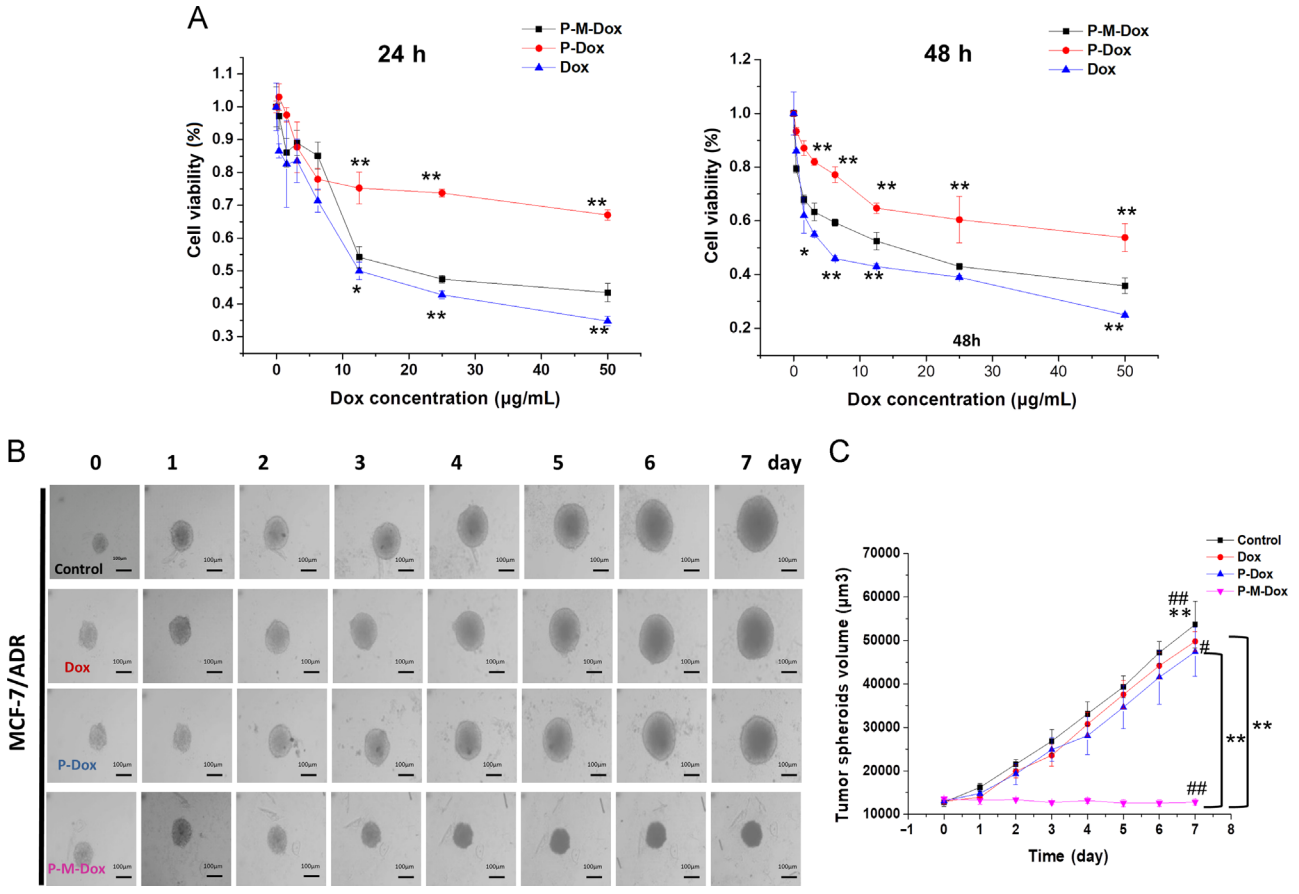

Figure 4 P-M-DOX overcomes drug resistance. (A) Viability of MCF-7/ADR cells after 24 or 48 h incubation with various concentrations of P-M-Dox, P-Dox and Dox. (B) Morphology and (C) volume of MCF-7/ADR tumor spheroids during the treatment. Scare bar: 100 μm. Results are mean ± SD, $n=3$. $^{\#}P<0.05$, $^{\#\#}P<0.01$ *versus* Dox group; $^{*}P<0.05$, $^{**}P<0.01$ *versus* P-M-Dox group.

could further protect payload from P-gp on the cell membrane. In consistence, the significant mitochondrial targeting of Dox delivered by P-M-Dox was accompanied with simultaneous promotion of ROS stimulation (Fig. 3D) and reduction of ATP generation (Fig. 3E), two important index of damaged mitochondria[59,60], as compared with free Dox and P-Dox.

3.3. *P-M-DOX overcomes drug resistance*

Given that ROS stress increment initiates cell apoptosis (*via* destroying the oxidative respiratory chain and activating caspase cascade reaction)[59,61], and insufficient ATP supply causes dysfunction of P-gp pumps, thus rendering resistant cells more susceptible, we further investigated the cell viability following P-M-Dox therapy. As expected, P-M-Dox (IC_{50}: 11.4 μg/mL, 48 h) showed superior cytotoxicity compared with P-Dox (IC_{50}: 56.82 μg/mL, 48 h) in MCF-7/ADR cells (Fig. 4A and Supporting Information Table S2). In addition, no cytotoxicity was observed for free MPP and HPMA copolymers (Supporting Information Fig. S2), which indicated the biosafety of carriers. Moreover, in MCF-7 cells, free Dox showed remarkable cytotoxicity, whereas its cytotoxicity was significantly reduced in drug-resistant MCF-7/ADR cells with resistance index (RI, IC_{50} value (in MCF7/ADR cells)/IC_{50} value (in MCF cells)) of 38.89 (Table S2). Results confirmed the prominent resistant nature of MCF-7/ADR cells. Although P-M-Dox showed slightly less inhibitory effect on cell proliferation compared with free Dox, it indeed displayed superior cytotoxicity against drug-resistant MCF-7/ADR cells compared with P-Dox. Moreover, several studies[24,62] reported similar results which might be related to the complexity of drug resistance mechanisms and different fate between polymeric conjugates and free molecules. Inspiringly, compared with free Dox, the level of resistance decreased from 38.89 to 4.37 and 2.45 for P-Dox and P-M-Dox treatments, respectively, suggesting that P-M-Dox has greater potential to defeat MDR. Although we observed above mentioned cell results, it should be stressed that P-M-Dox had the best inhibiting effect on 3D tumor spheroid model (Fig. 4B and C) that was closer to the condition of solid tumor, which showed the potential of macromolecular carriers and mitochondria targeting properties *in vivo*. In details, the quantitative volumes (Fig. 4C and Supporting Information Fig. S4) displayed the control group of HeLa, MCF-7, MCF-7/ADR tumor spheroids kept growing. However, the growth of tumor spheroid was suppressed after administrated with Dox, P-Dox and P-M-Dox. In details, P-M-Dox (96.02% of original spheroid volume at day 7) could reverse Dox resistance and exerted drastically better suppression in the spheroid

size than Dox (372.51% of original spheroid volume at day 7) and P-Dox (323.23% of original spheroid volume at day 7). Taken together, the data demonstrated the "two-pronged" strategy combining mitochondria targeting and macromolecular delivery was much more effective in overcoming multidrug resistance.

The platform applied herein demonstrated drug resistance could be overcome using P-M-Dox system, which exploited two important attributes: (1) macromolecular size of HPMA and (2) attachment of MPP.

In drug-resistant cells, P-gp is identified to actively pump drugs out of cells, which leads to low intracellular drug concentration, and consequently, the poor efficacy of chemotherapy. Recently, extensive efforts have been devoted to overcoming multidrug resistance by reducing P-gp mediated drug efflux. In this study, it was no surprise that free Dox showed less internalization and high efflux in the resistant MCF-7/ADR cells due to the overexpression of P-gp on the cell membrane, but this phenomenon could be tackled by P-M-Dox. Our findings demonstrated P-M-Dox system based on the macromolecular HPMA vehicle could endocytose into the cells and bypass the effect of P-gp mediated efflux, thereby improving the intracellular accumulation.

An additional feature of P-M-Dox system is mitochondria targeting which has been considered as another promising strategy to achieve effective antitumor efficacy even in drug-resistant cells. Once P-M-Dox entering cells through endocytosis, it responsively released M-Dox in endo/lysosome. In addition, as polymers with high molecular weight ($>$ 5 kDa) and hydrophilicity was difficult to pass through the mitochondria membrane[63], the detachment of M-Dox from HPMA copolymer was thus beneficial for mitochondria targeting. As compared with free Dox and P-Dox, P-M-Dox achieved more excellent mitochondria transportation due to MPP modification. Accordingly, the high mitochondria accumulation caused specific dysfunction of mitochondria with elevated ROS generation, which could impair vital cell components and activate cell apoptosis[64,65]. Furthermore, the higher ROS stress caused reduction of ATP production, thereby cutting off the energy supply for cell survival and suppressing the ATP-dependent "drug pump" function of P-gp, and eventually promoted the sensitivities of cancer cell to anticancer agents[66].

4. Conclusions

In summary, the modification of MPP and the application of HPMA copolymer endowed Dox with capability to surmount tumor drug resistance. On one hand, P-M-Dox with excellent mitochondrial targeting ability was found to achieve anti-MDR efficacy. This approach was not susceptible to individual differences in expression of MDR related gene or P-gp. On the other hand, the application of HPMA copolymers as carriers not only bypassed P-gp but also improved tumor specific accumulation *via* EPR effect for reduced side effects. Therefore, our platform might be applied as a promising anticancer drug delivery system to overcome tumor MDR. However, due to the restriction of the positive property of P-M-Dox, we conducted some preliminary studies including cytotoxicity and inhibition of 3D tumor spheroid assay to confirm the anti-MDR efficacy of P-M-Dox. In the future, a charge-reversal strategy[49,52] might be introduced to conceal the positive charge to avoid nonspecific protein absorption and rapid elimination by RES during circulation as well as guarantee the favorable cell internalization and mitochondria uptake at tumor site. Moreover, we might also expand the utility in other resistant cancer (*e.g.*, resistant human ovarian cancer) and combined other feasible approaches (*e.g.*, P-gp inhibitors, combination therapy) to combat MDR.

Acknowledgments

The authors gratefully acknowledge the financial support from the National Natural Science Foundation for Distinguished Young Scholars (81625023, China), the National Natural Science Foundation of China (81473167) and Sichuan Youth Science and Technology Innovation Research Team Funding (2016TD0001, China).

Appendix A. Supplementary information

Supplementary data associated with this article can be found in the online version at https://doi.org/10.1016/j.apsb.2018.11.005.

References

1. Chen WH, Luo GF, Qiu WX, Lei Q, Liu LH, Zheng DW, et al. Tumor-triggered drug release with tumor-targeted accumulation and elevated drug retention to overcome multidrug resistance. *Chem Mater* 2016;**28**:6742–52.
2. Cui W, Li J, Decher G. Self-assembled smart nanocarriers for targeted drug delivery. *Adv Mater* 2015;**28**:1302–11.
3. Pan L, Liu J, He Q, Shi J. MSN-mediated sequential vascular-to-cell nuclear-targeted drug delivery for efficient tumor regression. *Adv Mater* 2014;**26**:6742–8.
4. Szakács G, Paterson JK, Ludwig JA, Booth-Genthe C, Gottesman MM. Targeting multidrug resistance in cancer. *Nat Rev Drug Discov* 2006;**5**:219–34.
5. Torchilin VP. Multifunctional, stimuli-sensitive nanoparticulate systems for drug delivery. *Nat Rev Drug Discov* 2014;**13**:813–27.
6. Holohan C, van Schaeybroeck S, Longley DB, Johnston PG. Cancer drug resistance: an evolving paradigm. *Nat Rev Cancer* 2013;**13**:714–26.
7. Gottesman MM, Fojo T, Bates SE. Multidrug resistance in cancer: role of ATP-dependent transporters. *Nat Rev Cancer* 2002;**2**:48–58.
8. Aller SG, Yu J, Ward A, Weng Y, Chittaboina S, Zhuo R, et al. Structure of P-glycoprotein reveals a molecular basis for poly-specific drug binding. *Science* 2009;**323**:1718–22.
9. Mechetner E, Kyshtoobayeva A, Zonis S, Kim H, Stroup R, Garcia R, et al. Levels of multidrug resistance (MDR1) P-glycoprotein expression by human breast cancer correlate with *in vitro* resistance to taxol and doxorubicin. *Clin Cancer Res* 1998;**4**:389–98.
10. Hayes JD, Wolf CR. Molecular mechanisms of drug resistance. *Biochem J* 1990;**272**:281–95.
11. Ambudkar SV, Kimchi-Sarfaty C, Sauna ZE, Gottesman MM. P-glycoprotein: from genomics to mechanism. *Oncogene* 2003;**22**:7468–85.
12. Tang J, Zhang L, Gao H, Liu Y, Zhang Q, Ran R, et al. Co-delivery of doxorubicin and P-gp inhibitor by a reduction-sensitive liposome to overcome multidrug resistance, enhance anti-tumor efficiency and reduce toxicity. *Drug Deliv* 2016;**23**:1130–43.
13. To KK. MicroRNA: a prognostic biomarker and a possible druggable target for circumventing multidrug resistance in cancer chemotherapy. *J Biomed Sci* 2013;**20**:99.
14. Patel NR, Pattni BS, Abouzeid AH, Torchilin VP. Nanopreparations to overcome multidrug resistance in cancer. *Adv Drug Deliv Rev* 2013;**65**:1748–62.
15. Gandhi NS, Tekade RK, Chougule MB. Nanocarrier mediated delivery of siRNA/miRNA in combination with chemotherapeutic agents for cancer therapy: current progress and advances. *J Control Release* 2014;**194**:238–56.

16. Kathawala RJ, Gupta P, Ashby Jr CR, Chen ZS. The modulation of ABC transporter-mediated multidrug resistance in cancer: a review of the past decade. *Drug Resist Updates* 2015;**18**:1–17.
17. Ferry DR, Traunecker H, Kerr DJ. Clinical trials of p-glycoprotein reversal in solid tumours. *Eur J Cancer* 1996;**32**:1070–81.
18. Su CW, Chen SY, Liu DM. Polysaccharide-lecithin reverse micelles with enzyme-degradable triglyceride shell for overcoming tumor multidrug resistance. *Chem Commun* 2013;**49**:3772–4.
19. Park NH, Cheng W, Lai F, Yang C, de Sessions PF, Periaswamy B, et al. Addressing drug resistance in cancer with macromolecular chemotherapeutic agents. *J Am Chem Soc* 2018;**140**:4244–52.
20. Davis ME, Chen ZG, Shin DM. Nanoparticle therapeutics: an emerging treatment modality for cancer. *Nat Rev Drug Discov* 2008;**7**:771–82.
21. Gruenberg J. The endocytic pathway: a mosaic of domains. *Nat Rev Mol Cell Biol* 2001;**2**:721–30.
22. Markman JL, Rekechenetskiy A, Holler E, Ljubimova JY. Nanomedicine therapeutic approaches to overcome cancer drug resistance. *Adv Drug Deliv Rev* 2013;**65**:1866–79.
23. Gao Z, Zhang L, Sun Y. Nanotechnology applied to overcome tumor drug resistance. *J Control Release* 2012;**162**:45–55.
24. Minko T, Kopečková P, Pozharov V, Kopeček J. HPMA copolymer bound adriamycin overcomes *MDR1* gene encoded resistance in a human ovarian carcinoma cell line. *J Control Release* 1998;**54**:223–33.
25. Jiang L, Li L, He X, Yi Q, He B, Cao J, et al. Overcoming drug-resistant lung cancer by paclitaxel loaded dual-functional liposomes with mitochondria targeting and pH-response. *Biomaterials* 2015;**52**:126–39.
26. Xu RH, Pelicano H, Zhou Y, Carew JS, Feng L, Bhalla KN, et al. Inhibition of glycolysis in cancer cells: a novel strategy to overcome drug resistance associated with mitochondrial respiratory defect and hypoxia. *Cancer Res* 2005;**65**:613–21.
27. Han M, Vakili MR, Soleymani Abyaneh H, Molavi O, Lai R, Lavasanifar A. Mitochondrial delivery of doxorubicin *via* triphenylphosphine modification for overcoming drug resistance in MDA-MB-435/DOX cells. *Mol Pharm* 2014;**11**:2640–9.
28. Wang H, Gao Z, Liu X, Agarwal P, Zhao S, Conroy DW, et al. Targeted production of reactive oxygen species in mitochondria to overcome cancer drug resistance. *Nat Commun* 2018;**9**:562.
29. Zhou J, Zhao WY, Ma X, Ju RJ, Li XY, Li N, et al. The anticancer efficacy of paclitaxel liposomes modified with mitochondrial targeting conjugate in resistant lung cancer. *Biomaterials* 2013;**34**:3626–38.
30. Wang F, Sun W, Li L, Li L, Liu Y, Zhang ZR, et al. Charge-reversible multifunctional HPMA copolymers for mitochondrial targeting. *ACS Appl Mater Interfaces* 2017;**9**:27563–74.
31. Li L, Sun W, Li L, Liu Y, Wu L, Wang F, et al. A pH-responsive sequential-disassembly nanohybrid for mitochondrial targeting. *Nanoscale* 2016;**9**:314–25.
32. Lemasters JJ, Qian T, Kim JS, Elmore SP, Cascio WE, Brenner DA. Role of mitochondrial inner membrane permeabilization in necrotic cell death, apoptosis, and autophagy. *Antioxid Redox Signal* 2002;**4**:769–81.
33. Horton KL, Stewart KM, Fonseca SB, Guo Q, Kelley SO. Mitochondria-penetrating peptides. *Chem Biol* 2008;**15**:375–82.
34. Yousif LF, Stewart KM, Horton KL, Kelley SO. Mitochondria-penetrating peptides: sequence effects and model cargo transport. *Chembiochem* 2009;**10**:2081–8.
35. Kelley S, Pereira M, Fonseca S, inventors. Mitochondrial penetrating peptides as carriers for anticancer compounds. United States patent US 20130172266. 2011 May 27.
36. Li W, Zhang H, Assaraf YG, Zhao K, Xu X, Xie J, et al. Overcoming ABC transporter-mediated multidrug resistance: molecular mechanisms and novel therapeutic drug strategies. *Drug Resist Updates* 2016;**27**:14–29.
37. Ozben T. Mechanisms and strategies to overcome multiple drug resistance in cancer. *FEBS Lett* 2006;**580**:2903–9.
38. Kang L, Gao Z, Huang W, Jin M, Wang Q. Nanocarrier-mediated co-delivery of chemotherapeutic drugs and gene agents for cancer treatment. *Acta Pharm Sin B* 2015;**5**:169–75.
39. Yang X, Lyer AK, Singh A, Choy E, Hornicek FJ, Amiji MM, et al. MDR1 siRNA loaded hyaluronic acid-based CD44 targeted nanoparticle systems circumvent paclitaxel resistance in ovarian cancer. *Sci Rep* 2015;**5**:8509.
40. Li L, Sun W, Zhang Z, Huang Y. Time-staggered delivery of docetaxel and H1-S6A,F8A peptide for sequential dual-strike chemotherapy through tumor priming and nuclear targeting. *J Control Release* 2016;**232**:62–74.
41. Li L, Yang J, Wang J, Kopeček J. Amplification of CD20 cross-linking in rituximab-resistant B-lymphoma cells enhances apoptosis induction by drug-free macromolecular therapeutics. *ACS Nano* 2018;**12**:3658–70.
42. Li L, Yang J, Wang J, Kopeček J. Drug-free macromolecular therapeutics induce apoptosis *via* calcium influx and mitochondrial signaling pathway. *Macromol Biosci* 2017;**18**:1700196.
43. Basavaraj S, Betageri GV. Can formulation and drug delivery reduce attrition during drug discovery and development—review of feasibility, benefits and challenges. *Acta Pharm Sin B* 2014;**4**:3–17.
44. Etrych T, Mrkvan T, Chytil P, Koňák Č, Říhová B, Ulbrich K. *N*-(2-hydroxypropyl)methacrylamide-based polymer conjugates with pH-controlled activation of doxorubicin. I. New synthesis, physicochemical characterization and preliminary biological evaluation. *J Appl Polym Sci* 2008;**109**:3050–61.
45. Omelyanenko V, Kopečková P, Gentry C, Kopeček J. Targetable HPMA copolymer-adriamycin conjugates. Recognition, internalization, and subcellular fate. *J Control Release* 1998;**53**:25–37.
46. Meyer dos Santos S, Weber CC, Franke C, Müller WE, Eckert GP. Cholesterol: coupling between membrane microenvironment and ABC transporter activity. *Biochem Biophys Res Commun* 2007;**354**:216–21.
47. Sivak L, Subr V, Tomala J, Rihova B, Strohalm J, Etrych T, et al. Overcoming multidrug resistance *via* simultaneous delivery of cytostatic drug and P-glycoprotein inhibitor to cancer cells by HPMA copolymer conjugate. *Biomaterials* 2017;**115**:65–80.
48. Bass DA, Parce JW, Dechatelet LR, Szejda P, Seeds MC, Thomas M. Flow cytometric studies of oxidative product formation by neutrophils: a graded response to membrane stimulation. *J Immunol* 1983;**130**:1910–7.
49. Li L, Yang Q, Zhou Z, Zhong J, Huang Y. Doxorubicin-loaded, charge reversible, folate modified HPMA copolymer conjugates for active cancer cell targeting. *Biomaterials* 2014;**35**:5171–87.
50. Vinci M, Gowan S, Boxall F, Patterson L, Zimmermann M, Court W, et al. Advances in establishment and analysis of three-dimensional tumor spheroid-based functional assays for target validation and drug evaluation. *BMC Biol* 2012;**10**:29.
51. Gianasi E, Wasil M, Evagorou EG, Keddle A, Wilson G, Duncan R. HPMA copolymer platinates as novel antitumour agents: *in vitro* properties, pharmacokinetics and antitumour activity *in vivo*. *Eur J Cancer* 1999;**35**:994–1002.
52. Li L, Sun W, Zhong J, Yang Q, Zhu X, Zhou Z, et al. Multistage nanovehicle delivery system based on stepwise size reduction and charge reversal for programmed nuclear targeting of systemically administered anticancer drugs. *Adv Funct Mater* 2015;**25**:4101–13.
53. Alta RY, Vitorino HA, Goswami D, Liria CW, Wisnovsky SP, Kelley SO, et al. Mitochondria-penetrating peptides conjugated to desferrioxamine as chelators for mitochondrial labile iron. *PLoS One* 2017;**12**:e0171729.
54. Shieh MJ, Hsu CY, Huang LY, Chen HY, Huang FH, Lai PS. Reversal of doxorubicin-resistance by multifunctional nanoparticles in MCF-7/ADR cells. *J Control Release* 2011;**152**:418–25.
55. Thomas H, Coley HM. Overcoming multidrug resistance in cancer: an update on the clinical strategy of inhibiting p-glycoprotein. *Cancer Control* 2003;**10**:159–65.
56. Bareford LM, Swaan PW. Endocytic mechanisms for targeted drug delivery. *Adv Drug Deliv Rev* 2007;**59**:748–58.

57. Battistella C, Klok HA. Reversion of P-gp-mediated drug resistance in ovarian carcinoma cells with PHPMA-zosuquidar conjugates. *Biomacromolecules* 2017;**18**:1855–65.
58. Minko T. HPMA copolymers for modulating cellular signaling and overcoming multidrug resistance. *Adv Drug Deliv Rev* 2010;**62**:192–202.
59. Gogvadze V, Orrenius S, Zhivotovsky B. Mitochondria in cancer cells: what is so special about them?. *Trends Cell Biol* 2008;**18**:165–73.
60. Zong WX, Rabinowitz JD, White E. Mitochondria and cancer. *Mol Cell* 2016;**61**:667–76.
61. Indran IR, Tufo G, Pervaiz S, Brenner C. Recent advances in apoptosis, mitochondria and drug resistance in cancer cells. *Biochim Biophys Acta* 2011;**1807**:735–45.
62. Šťastný M, Strohalm J, Plocová D, Ulbrich K, Říhová B. A possibility to overcome P-glycoprotein (PGP)-mediated multidrug resistance by antibody-targeted drugs conjugated to *N*-(2-hydroxypropyl)methacrylamide (HPMA) copolymer carrier. *Eur J Cancer* 1999;**35**:459–66.
63. Kroemer G, Galluzzi L, Brenner C. Mitochondrial membrane permeabilization in cell death. *Physiol Rev* 2007;**87**:99–163.
64. Ott M, Gogvadze V, Orrenius S, Zhivotovsky B. Mitochondria, oxidative stress and cell death. *Apoptosis* 2007;**12**:913–22.
65. Kroemer G, Reed JC. Mitochondrial control of cell death. *Nat Med* 2000;**6**:513–9.
66. Pelicano H, Carney D, Huang P. ROS stress in cancer cells and therapeutic implications. *Drug Resist Updates* 2004;**7**:97–110.